

# Three-dimensional and molecular analysis of the arterial pole of the developing human heart

Aleksander Sizarov,<sup>1</sup> Wouter H. Lamers,<sup>2</sup> Timothy J. Mohun,<sup>3</sup> Nigel A. Brown,<sup>4</sup> Robert H. Anderson<sup>5</sup> and Antoon F. M. Moorman<sup>1</sup>

<sup>1</sup>Department of Anatomy, Embryology & Physiology, Academic Medical Center, Amsterdam, the Netherlands

<sup>2</sup>Tytgat Institute for Liver and Intestinal Research, Academic Medical Center, Amsterdam, the Netherlands

<sup>3</sup>Division of Developmental Biology, MRC National Institute for Medical Research, London, UK

<sup>4</sup>Division of Biomedical Sciences, St George's University of London, UK

<sup>5</sup>Institute of Human Genetics, Newcastle University, Newcastle upon Tyne, UK

## Abstract

Labeling experiments in chicken and mouse embryos have revealed important roles for different cell lineages in the development of the cardiac arterial pole. These data can only fully be exploited when integrated into the continuously changing morphological context and compared with the patterns of gene expression. As yet, studies on the formation of separate ventricular outlets and arterial trunks in the human heart are exclusively based on histologically stained sections. So as to expand these studies, we performed immunohistochemical analyses of serially sectioned human embryos, along with three-dimensional reconstructions. The development of the cardiac arterial pole involves several parallel and independent processes of formation and fusion of outflow tract cushions, remodeling of the aortic sac and closure of an initial aortopulmonary foramen through formation of a transient aortopulmonary septum. Expression patterns of the transcription factors ISL1, SOX9 and AP2 $\alpha$  show that, in addition to fusion of the SOX9-positive endocardial cushions, intrapericardial protrusion of pharyngeal mesenchyme derived from the neural crest contributes to the separation of the developing ascending aorta from the pulmonary trunk. The non-adjacent walls of the intrapericardial arterial trunks are formed through addition of ISL1-positive cells to the distal outflow tract, while the facing parts of the walls form from the protruding mesenchyme. The morphogenetic steps, along with the gene expression patterns reported in this study, are comparable to those observed in the mouse. They confirm the involvement of mesenchymal tissues derived from endocardium, mesoderm and migrating neural crest cells in the process of initial septation of the distal part of the outflow tract, and its subsequent separation into discrete intrapericardial arterial trunks.

**Key words:** aortic arches; heart development; human embryo; outflow tract.

## Introduction

Malformations of the arterial pole of the heart, encompassing the ventricular outlets and arterial trunks, constitute almost one-third of all cardiac malformations (Hoffman & Kaplan, 2002), and are often incompatible with life without intervention (Samánek, 1992). The malformations are markedly diverse, combining abnormalities in ventriculo-arterial connections and septation, along with valvar and vascular

defects. This strongly suggests an intimate association of separate morphogenetic and molecular pathways in the formation of the structures making up the outflow tract. The desire to discover the morphogenetic mechanisms underlying the malformations spawned a multitude of studies. These studies, however, in turn produced a plethora of terms used to describe the components of the developing outflow tract, as summarised in the recent comprehensive review made by Okamoto et al. (2010). The diversity of terminology has made the existing literature quite inaccessible, even for the morphological expert.

Studies of the shaping and septation of the outflow tract in experimental animals, nonetheless, have revealed crucial roles for mesenchymal tissues derived from the neural crest and the second heart field (Farrell et al. 1999; Dyer & Kirby, 2009), albeit thus far with limited integration of the molecular and lineage analyses into the complex three-dimensional

### Correspondence

Antoon F. M. Moorman, Department of Anatomy, Embryology & Physiology, Academic Medical Center, Meibergdreef 15, 1105AZ Amsterdam, the Netherlands. T: +31 20 5664928; F: +31 20 6976177; E: a.f.moorman@amc.uva.nl

Accepted for publication 30 December 2011

Article published online 1 February 2012

(3D) context of the outflow tract. Studies in the human, however, have thus far been based only on histologically stained sections, and have produced conflicting interpretations, particularly regarding the mechanism of the so-called aortopulmonary septation. Based on the studies by Tandler (1912), during the first half of the previous century it had been believed (Kramer, 1942) that the role of the aortopulmonary septum, later called aortico-pulmonary septum (van Mierop et al. 1963), was well understood. Despite that, studies in the second half of the previous century, while using the same methodology, have introduced the controversial concept of the so-called 'aortopulmonary septal complex' (Thompson et al. 1985). To obtain further insight into the intricate morphological changes occurring within the distal component of the human outflow tract, we have performed an integrated molecular and 3D analysis of the tissues involved in the separation of the single outflow tract into systemic and pulmonary arterial channels. The morphogenetic steps, along with the gene expression patterns reported in this study, are comparable to those observed in the mouse (our own unpublished observations), lending support to the veracity of extrapolations of the mechanisms governing development of the arterial pole derived from experimental studies to the human.

## Materials and methods

### Human embryos

Collection of human embryonic material and preparation for histological studies were described previously (Sizarov et al. 2010). In total, we used seven embryos at Carnegie stages 12 and 13, five at stages 14 and 15, five at stage 16, four at stage 18, and three at stages 21–23. We included only embryos considered normal. Collection, and use, of the human embryonic material for research was approved by the Medical Ethical Committees of the Universities of Tartu, Estonia and Amsterdam, the Netherlands. In addition, high-resolution episcopic microscopy (Weninger & Mohun, 2007) was applied to 14 embryos at stages 13–18. These embryos, which were judged as unsuitable for gene expression studies, were kindly provided by the MRC–Wellcome Trust Human Developmental Biology Resource (<http://www.hdb.org>), managed by the Institute for Human Genetics of Newcastle University, UK.

### Triple-fluorescent immunohistochemistry

Paraffin-embedded embryos were sectioned at 7–10  $\mu\text{m}$ . Triple-immunofluorescent staining was performed as described previously (Sizarov et al. 2010). Here we report the results of staining with the following primary antibodies: goat polyclonal for connexin40; rabbit polyclonal for NKX2-5 (both from Santa Cruz Biotechnology, Santa Cruz, CA, USA; diluted 1 : 250); goat polyclonal for Islet-1 (1 : 250; Neuromics, Edina, MN, USA); rabbit polyclonal for SOX9 (1 : 250; Chemicon, Millipore, Billerica, MA, USA); rabbit polyclonal for Ki67 (1:500; Monosan, Uden, the Netherlands); mouse monoclonal for  $\alpha$ -smooth muscle actin (1 : 500; Sigma-Aldrich, St. Louis, MO, USA); and mouse

monoclonal for AP2 $\alpha$  (1 : 25; Developmental Studies Hybridoma Bank, University of Iowa, Iowa City, IA, USA). Some combinations of primary antibodies contained a mouse monoclonal antibody for troponin I (1 : 250; Chemicon) as myocardial marker. After incubation overnight and washing, sections were incubated for 1.5–2 h with a mix of fluorochrome-coupled secondary antibodies containing donkey-anti-goat Alexa568, chicken-anti-rabbit Alexa488 and donkey-anti-mouse Alexa680 (all diluted 1 : 250; Molecular Probes, Invitrogen, Eugene, OR, USA).

### Three-dimensional reconstructions

Three-dimensional reconstructions from the fluorescently stained serial sections were performed using Amira software (<http://www.amiravis.com>), essentially as described previously (Sizarov et al. 2010). Myocardium was labeled on basis troponin I expression. The labels for other structures, which were not specifically stained, were defined according to general embryological knowledge (Gasser, 1975; O'Rahilly & Müller, 1987). Some structures (e.g. pharyngeal mesenchyme, coelomic wall, veins and arteries) were not labeled in their entirety for the sake of clarity. The 3D data from the Amira viewer were exported into Adobe Acrobat 9 Pro Extended (Adobe Systems, <http://www.adobe.com>) to generate the files in an interactive 3D portable document format (de Boer et al. 2011).

### Preparation of the models using high-resolution episcopic microscopy

Episcopic datasets were prepared as previously described (Weninger & Mohun, 2007), with minor modifications. Human embryos were dehydrated through graded methanol and infiltrated for 24–48 h with JB-4 methacrylate embedding solution (Polysciences, Warrington, PA, USA) supplemented with 0.27% eosin and 0.06% acridine orange. The same mix was used for polymerisation using the manufacturer's protocol, except that 50% more catalyst was employed. After polymerisation, blocks were sectioned at 2–3  $\mu\text{m}$  and successive block face images captured using a Hamamatsu Orca HR CCD camera attached to Olympus MVX optics, with GFP excitation and emission filters. Sectioning and image capture were automated via Image Pro 6 software (Media Cybernetics, Bethesda, MD, USA). Gray levels of raw datasets were adjusted to provide optimal tissue contrast using Photoshop CS3 (Adobe Systems). For 3D volume rendering, the heart region of each embryo was sub-sampled to a final dataset size of 250–300 Mb, inverted and rendered using Osirix 3.8 (<http://www.osirix-viewer.com>).

### Limitations of our study

Assessment of cellular lineage should ideally be performed by means of genetic or physical labeling of cells, a technique clearly impossible in human embryos. The second best option is to study patterns of gene expression. A particular limitation here is that neural crest-derived cells expressing the DNA-binding activator protein AP2 $\alpha$  (Brewer et al. 2002; Betters et al. 2010) could only be detected during their migration. Stainings for other known neural crest molecular markers (Betters et al. 2010) were not successful. The non-standardised fixation, and limited numbers of available embryos, did not permit complete optimisation of the staining protocol for some antibodies, and

prevented assessment of biological variation between specimens at similar developmental stages. Despite these potential problems, immunohistochemical stainings proved to be reproducible. The use of the episcopic microscopy allows exquisite assessment of the internal morphology in almost any desired section plane but, in the human embryo, does not readily permit the distinction between tissue types.

## Results

We define the outflow tract as the outlet portion of the developing heart contained within the coelomic, or pericardial, cavity. From stage 12 onward, the outflow tract is a distinct morphological entity within the developing heart, as will be discussed below. It is, however, a highly dynamic structure, with differentiating cells continuously added distally from the pharyngeal mesoderm (Cai et al. 2003; Buckingham et al. 2005; Dyer & Kirby, 2009), and with cells seemingly 'disappearing' proximally through differentiation into right ventricular myocardium (de la Cruz et al. 1977; Rana et al. 2007). From the stance of lineage, therefore, it is likely that the components of the developing outflow tract at each of the stages studied here are composed of different cells when compared with the preceding stage.

The curved and changing nature of the pharyngeal region encompassing the cardiac outflow tract (Fig. 1) produces difficulties in describing the components of the outflow tracts using terms such as ventral and dorsal, or cranial and caudal in describing the location of the structures making up the outflow tract. For the sake of simplicity, the structures located close to the developing spine on a transverse section are called dorsal, and those extending toward the developing brain are named cranial, with the opposite coordinates considered ventral and caudal, respectively. To facilitate the understanding of the complex morphogenetic changes encountered, we encourage the reader to examine the results along with the interactive 3D-PDF file provided

in the online Supporting information, Data S1 (accessible at <http://onlinelibrary.wiley.com>).

## Stages 12 and 13 – the tubular outflow tract and aortic sac

In the looped and chamber-forming heart at stages 12 and 13, which corresponds to 26–30 days of development, it is possible to recognise a venous sinus, left and right atrial pouches, an atrioventricular canal, left and right ventricles and a tubular outflow tract (Fig. 2A–C). At this early stage, the outflow tract is entirely myocardial, and forms a serpentine-like connection between an inconspicuous dorso-caudally located right ventricle and the aortic sac, which is embedded within the pharyngeal mesenchyme and gives rise to three pairs of symmetric aortic arch arteries (Fig. 2A–C). The myocardial wall of the outflow tract is contiguous with the epithelial lining of the coelomic cavity and expresses ISL1 (Fig. 2E,H), a marker of the cardiac progenitor cells within the heart-forming regions (Cai et al. 2003). The lumen of the outflow tract is bordered by endocardium expressing connexin40 (Fig. 2F,G). Between the endocardium and myocardium, the cardiac jelly contains sparse mesenchymal cells expressing the transcription factor SOX9 (Fig. 2I), indicating their endocardial origin through endothelial–mesenchymal transformation (Akiyama et al. 2004). There is no indication of septation, with the lumen of the intrapericardial outflow tract continuing extrapericardially as the aortic sac and aortic arches (Fig. 2C–E). The lumens of the right and left pulmonary arteries take origin from the proximal part of the paired sixth aortic arches, running caudally within the pharyngeal mesenchyme (Fig. 2D). At stage 13, we observed the first indication of ISL1-positive mesenchymal tissue indenting the most distal aspect of the outflow tract (Fig. 2G,H). This mesenchymal tissue later takes the form of two column-like structures, which become more clearly distinguishable during stages 14 and 15. The

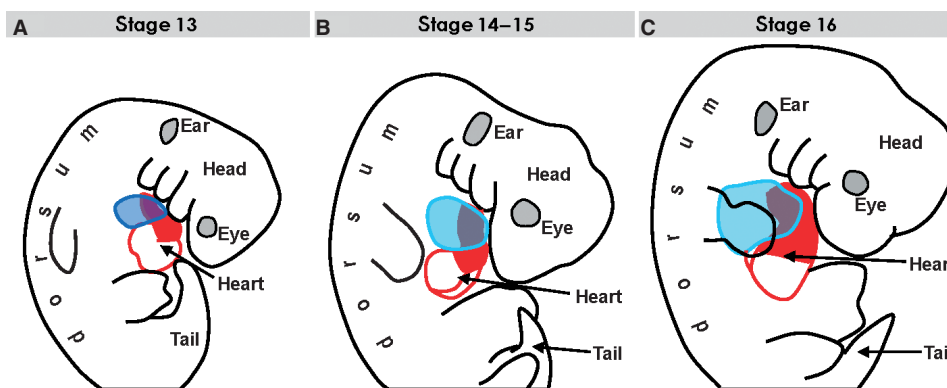


**Fig. 1** The contours of the developing heart (red and blue lines) superimposed on the silhouettes of embryos at consecutive stages to illustrate the ambiguity of terms 'dorsal/ventral' and 'cranial/caudal' in describing the morphogenesis of the curved and changing pharyngeal region. (A) The contour of the stage 13 embryo, the reconstructed heart of which is shown in Fig. 2. (B) Stage 15 embryo (see Fig. 3). (C) Stage 16 embryo (see Fig. 6).



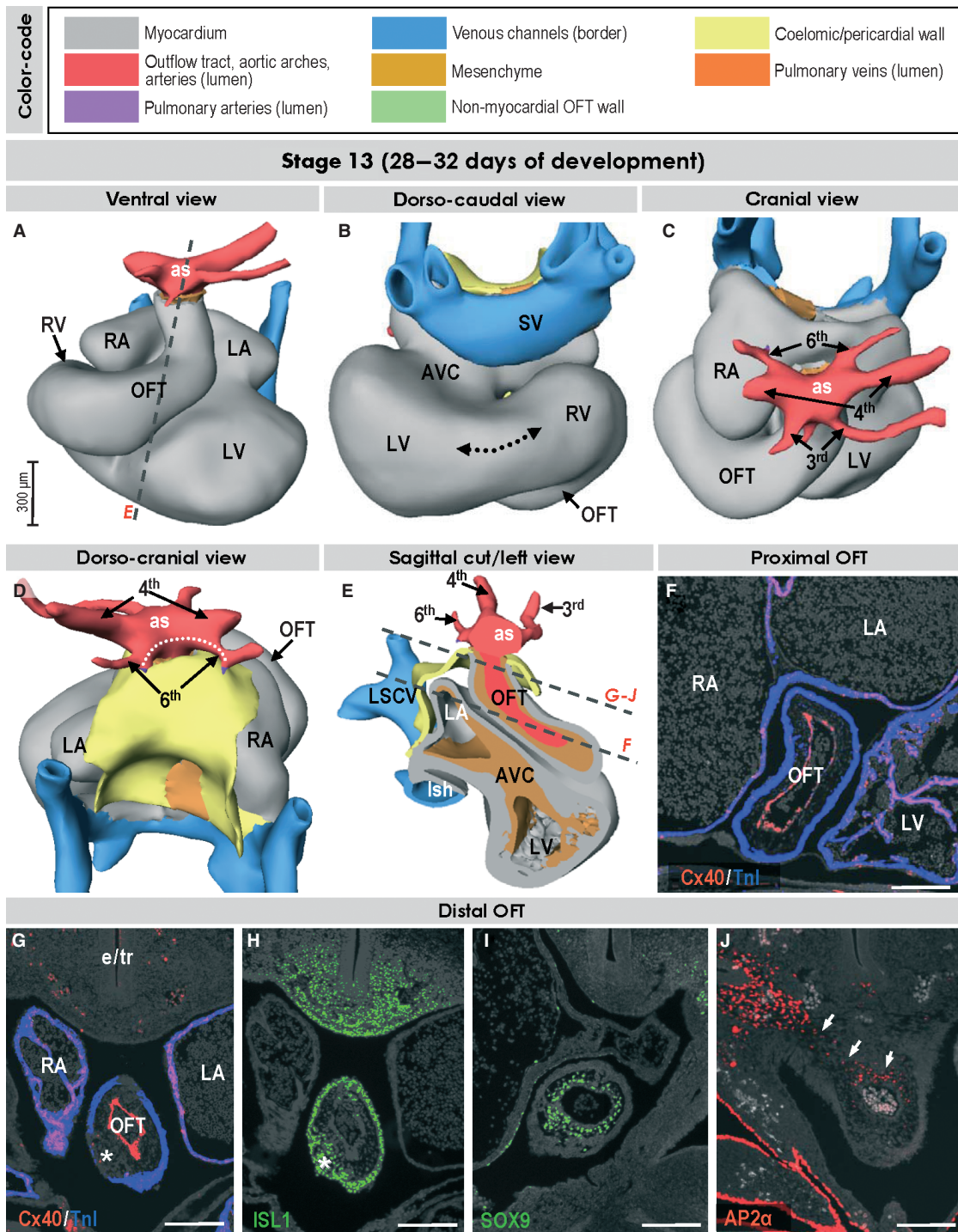


**Fig. 2** Three-dimensional (3D) and molecular analysis of the cardiac outflow tract at stage 13. (A–E) At this stage the myocardial outflow tract (OFT), connecting the right ventricle with the aortic sac (as), is tubular and its lumen is lined by connexin40-positive endocardium (F,G). The 3rd, 4th and 6th aortic arches originate directly from the aortic sac. The dotted line in (D) refers to the distance between the origins of tiny right and left pulmonary arteries. Note the canal-like part of the looping heart tube interposed between the ballooning left and right ventricles (dotted line in B). (G–J) Sections through the distal outflow tract, which were incubated with antibodies as indicated. The asterisks in (G) and (H) point to the appearance of mesenchymal tissue within the distal outflow tract taking the form of columns at later stages (see text). The small arrows in (J) point to contiguity between neural crest-derived cells of outflow tract and pharyngeal mesenchyme. Scale bars: 200 µm. Abbreviations: AVC, atrioventricular canal; e/tr, (undivided) developing esophagus and trachea; LA/RA, left/right atrium; LSCV, left superior cardinal vein; Lsh, left sinus horn; LV/RV, left/right ventricle; SV, sinus venosus.



expression of AP2 $\alpha$ , a transcription factor expressed in migrating cells derived from the cardiac neural crest (Brewer et al. 2002), indicates already the presence of these cells within the outflow tract (Fig. 2J).

### Stages 14 and 15 – septation of the proximal outflow tract and remodeling of the aortic sac

At stages 14 and 15, which correspond to 31–36 days of development, the outflow tract has become relatively shorter, concomitant with the ventricularisation of its proximal part (de la Cruz et al. 1977; Rana et al. 2007; Fig. 3A). The cells making up its myocardial wall continue to express ISL1 (Fig. 3I). The mesenchyme within the proximal part of the outflow tract has now become more densely populated, forming a pair of cushions (asterisks in Fig. 3E), which approximate each other to divide the lumen into prospective aortic and pulmonary channels, connecting the right ventricular cavity and the primary interventricular foramen with the distal outflow tract in a slightly spiral fashion (dotted lines in Fig. 3D). The distal part of the outflow tract is still undivided at this stage, and resembles the tubular outflow tract as seen in the stage 13 heart (Fig. 3D,F). Its distal myocardial wall is still contiguous with the epithelial lining of the coelomic cavity. The myocardial component shows virtual lack of proliferation (Fig. 3H), as previously reported for the rat (Ya et al. 1998). The lumen of the distal outflow tract, however, now continues extrapericardially as a longitudinal arterial channel, which is about four times narrower than the original aortic sac (Fig. 3C,D). Similar to previous reports (van Mierop et al. 1963; Orts-Llorca et al. 1982), we consider this arterial channel to represent the future extrapericardial ascending aorta. The sixth aortic arches, giving rise to the right and left branches of the pulmonary arteries, originate from the caudal aspect of the junction between distal outflow tract and developing ascending aorta, from which the fourth and third arches arise more cranially (Fig. 3A–D). At this stage, however, both the forming distal aortic and pulmonary channels originate from the lumen of the unseptated distal part of the outflow tract, the most distal end of which we consider as an aortopulmonary foramen.

The mesenchyme of the pharyngeal region bordering the distal outflow tract is molecularly diverse. Dorsally, the unseptated distal outflow tract is bordered by the ISL1-positive pharyngeal mesenchyme (Fig. 3I), which is interposed between the origins of the symmetric sixth and fourth pairs of aortic arches (star in Fig. 4A,A\*,A\*\*). Similar to previous interpretations (Tandler, 1912; Kramer, 1942), we consider this tissue, which on sagittal cuts slightly protrudes into the lumen of the distal outflow tract, as the first sign of aortopulmonary septation. AP2 $\alpha$ -positive cells are seen along the sixth aortic arches, and ventral to the ISL1-positive protruding mesenchyme (Fig. 3K), suggesting the route of migration of cells derived from the neural

crest (Farrell et al. 1999). As AP2 $\alpha$  is no longer expressed in the non-migrating neural crest-derived cells, these cells are not seen in the SOX9-positive endocardial cushions of the proximal outflow tract (not shown). At the ventral and dorsal aspects of the distal outflow tract the pharyngeal mesenchymal tissue expressing ISL1 is now clearly recognisable as taking the form of two non-myocardial column-like structures (Fig. 3A,B). These mural structures, only briefly mentioned in previous reports (Kramer, 1942; de Vries & de Saunders, 1962; Thompson et al. 1985), are in direct continuity with the ISL1-positive pharyngeal mesenchyme, and interdigitate with the endocardium-derived mesenchyme, as well as with the myocardial wall of the distal outflow tract (Fig. 3F–K). The mesenchyme making up these column-like structures is devoid of SOX9, AP2 $\alpha$  and  $\alpha$ -smooth muscle actin ( $\alpha$ SMA), and shows virtually no proliferation. The endocardially derived mesenchyme covering the columns, in contrast, is SOX9-,  $\alpha$ SMA- and Ki67-positive (Fig. 3G–J). The non-myocardial columns extend intrapericardially into the intermediate part of the outflow tract, where they are surrounded by the myocardial wall of the outflow tract and can be seen to presage the appearance of the intercalated cushions (Fig. 5A–D), which are more clearly evident at the next stage.

### Stage 16 – septation of the distal outflow tract

At stage 16, thus 4–6 days later, the myocardial part of the outflow tract hardly expresses ISL1 (Fig. 6I) and has shortened further, whereas the mass of the right ventricle has become visible ventrally (Fig. 6A). The endocardial cushions expressing SOX9 are now formed also within the distal part of the outflow tract (Fig. 6J,K). The approximation of these cushions to each other divides the lumen of the distal outflow tract into the future aortic and pulmonary channels, the spiral orientation of which (dotted lines in Fig. 6D) already reflecting the definitive postnatal topographic relations (Webb et al. 2003). The most distal lumen of the outflow tract, the aortopulmonary foramen, is now also septated through progressive intrapericardial protrusion of the dorsal pharyngeal mesenchyme (Fig. 4B,B\*,B\*\*). This moderately proliferating mesenchyme, which forms a transient aortopulmonary septum (Tandler, 1912; Kramer, 1942; van Mierop et al. 1963; Orts-Llorca et al. 1982; Beall & Rosenquist, 1990), is ISL1- and SOX9-negative, and expresses AP2 $\alpha$  (Fig. 6H–K), suggesting that migration of neural crest-derived cells ventral to the ISL1-positive pharyngeal tissues is involved in driving the protrusion. The protruding mesenchyme is strongly positive for  $\alpha$ SMA (Fig. 6G). Intrapericardially, the septum is obliquely positioned between the separating aortic and pulmonary channels, with the pulmonary trunk extending leftward from the midline and the developing ascending aorta positioned to the right (Fig. 6B,C). The pulmonary trunk continues extrapericardially as the pair of the sixth aortic arches, from which arise the

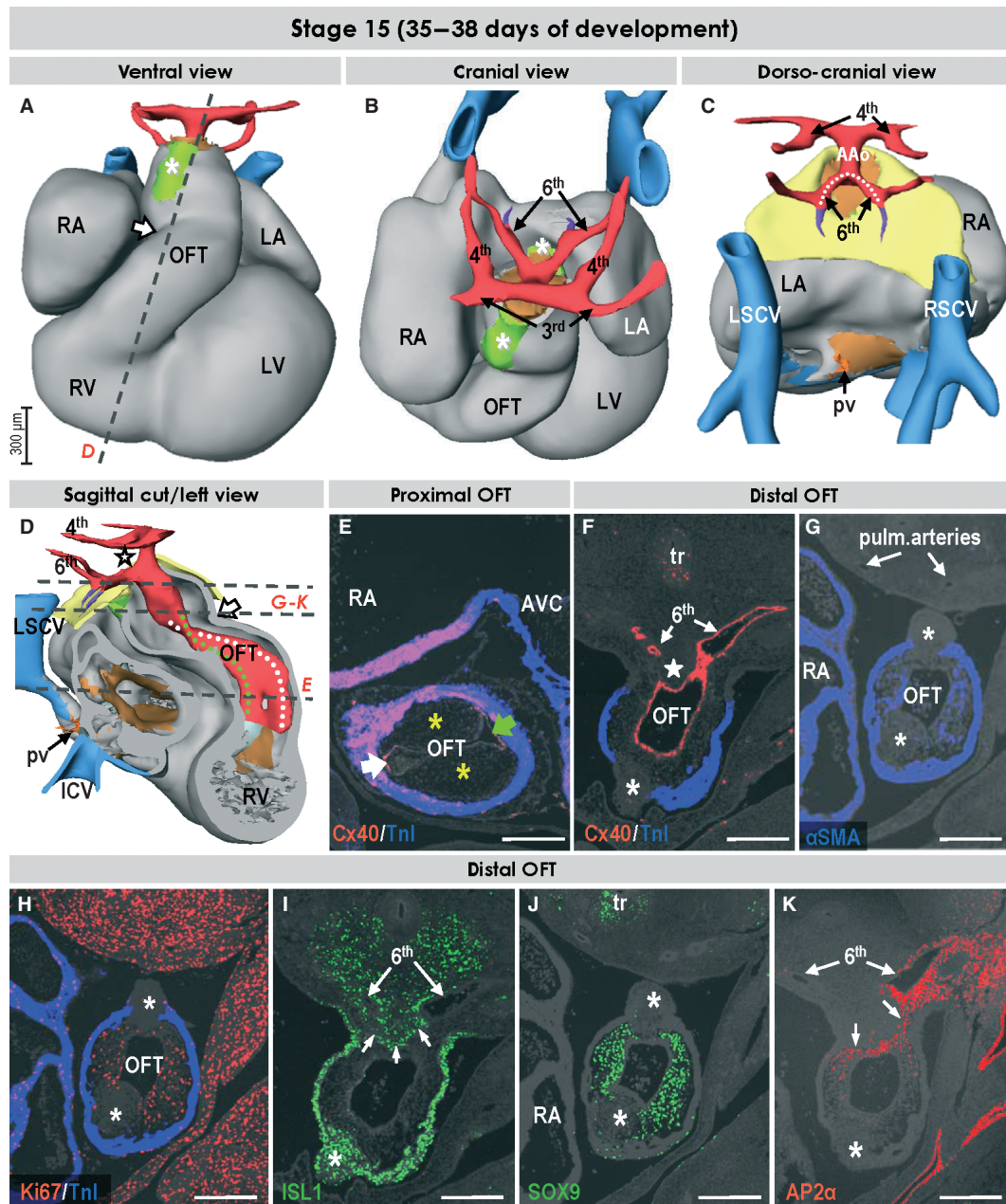


**Fig. 3** Three-dimensional (3D) and molecular analysis of the cardiac outflow tract at stage 15. (A–D) The intrapericardial mesenchymal tissue forming the column-like structures at ventral and dorsal aspects of the distal outflow tract (asterisks in A and B). Note the appearance of the longitudinal arterial channel, the future ascending aorta (AAo) giving rise to the 3<sup>rd</sup> and 4<sup>th</sup> aortic arches. The 6<sup>th</sup> aortic arches originate separately from the unseptated distal outflow tract (E) as the result of the remodeling of the aortic sac. The dotted line in (C) points to the decreasing distance between the origins of the left and right pulmonary arterial branches. The arrows in (A) and (D) point to the characteristic bend of the myocardial outflow tract, dividing it into proximal and distal parts. Dotted lines in (D) refer to the spirally oriented channels in the proximal outflow tract connecting the unseptated distal outflow tract with the right ventricle (white line) and the primary interventricular foramen (green line). (E) Section through the proximal outflow tract showing the unfused endocardial cushions producing aortic and pulmonary arterial channels (green and white arrows, respectively). (F–J) Sections through the distal outflow tract, which were incubated with antibodies, as indicated. The star in (F) points to the mesenchyme located between the 4<sup>th</sup> and 6<sup>th</sup> and between the right and left aortic arches. Asterisks in (F)–(K) point to the ventrally and dorsally located columns of mesenchymal tissue (see text). Scale bars: 200 μm. Abbreviations: pv, pulmonary vein; tr, trachea; for other abbreviations, see Fig. 1.

left and right pulmonary arteries, while the third and fourth aortic arches originate symmetrically from the extrapericardial portion of the ascending aorta (Fig. 6A–C).

The non-myocardial walls of the distal outflow tract bordering laterally the future intrapericardial arterial trunks are ISL1- and αSMA-positive, but do not express AP2α



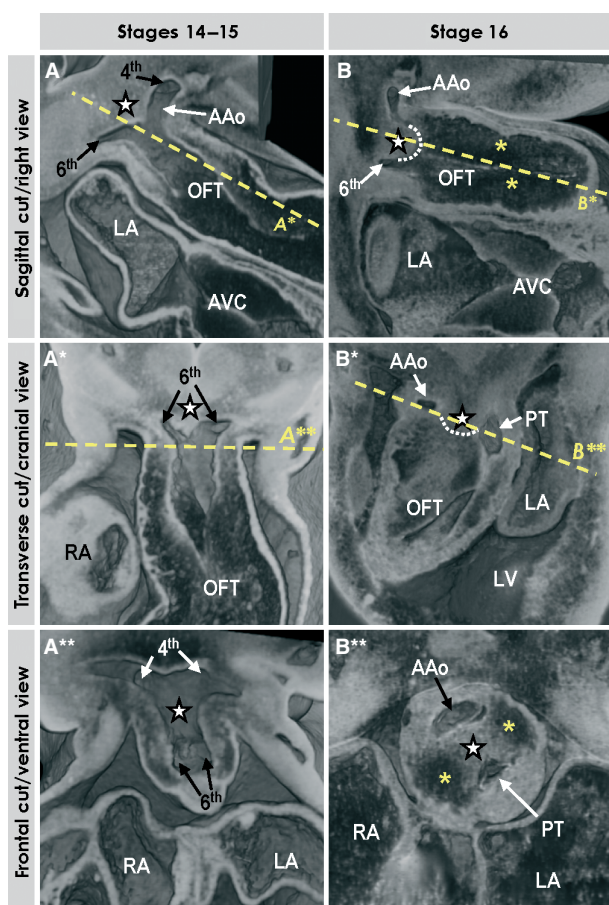


**Fig. 4** Three-dimensional (3D) morphology of the distal outflow tract, as assessed by high-resolution episcopic microscopy. (A–A\*\*) Different views of the unseptated distal outflow tract at stages 14–15 with the dorsal wall between the 4th and 6th aortic arches slightly protruding intrapericardially (star), which leads to the appearance of the future extrapericardial ascending aorta (AAo). (B–B\*\*) Different views through the septated distal outflow tract at stage 16. Note that progressive protrusion of the dorsal wall of the outflow tract intrapericardially leads to the formation of the so-called aortopulmonary septum (#, outlined by the dotted line in B, B\*) separating the developing intrapericardial aortic channel from the future pulmonary trunk (PT). Yellow asterisks indicate endocardial cushions. See text for further description.

(Fig. 6F,G,I,K). AP2 $\alpha$ , however, is expressed in the mesenchyme surrounding the aortic arch arteries, supporting the notion of a distinct developmental origin of the non-facing walls of intrapericardial arterial trunks and the arterial channels arising from them (Bergwerff et al. 1998).

The ISL1-positive mesenchymal column-like components within the wall of the distal outflow tract wall, clearly discernible ventrally and dorsally at earlier stages, are no longer identifiable at this stage. In the middle and distal portions of the outflow tract, however, small intercalated cushions, or swellings (Kramer, 1942), of an almost triangular shape on a cross-section are now visible opposing one

another along the systemic and pulmonary arterial channels (Fig. 5E–H). The tissue of the intercalated cushions is weakly ISL1-positive and expresses moderately SOX9, suggesting invasion of endocardium-derived cells into the intercalated cushions (Fig. 5F,G). As previously shown for rat (Ya et al. 1998), the intercalated cushions are virtually devoid of the  $\alpha$ SMA expression (Fig. 5H). The appearance of these intercalated cushions along with the other two cushions presages the formation of the arterial valves (Kramer, 1942; Maron & Hutchins, 1974).

### Stages 18–23 – formation of the intrapericardial arterial trunks

After another 5–7 days, at stage 18, the cardiac outflow tract is configured as for the postnatal heart, with the distal intrapericardial outflow tract now separated into discrete aortic and pulmonary components (Fig. 7A,B,C,E). The distal border of the myocardial component, however, continues at this stage to surround the developing arterial valves, while its proximal part forms the non-proliferating myocardial walls of both ventricular outlets (Fig. 7D–F). The mesenchymal tissue between the proximal right and left ventricular outflow tracts (asterisk in Fig. 7C,D) begins to myocardialise (van den Hoff et al. 1999). The most distal intrapericardial portion of the outflow tract now constitutes the arterial trunks, which spiral slightly round one another (Fig. 7A–C), and have separate walls strongly expressing  $\alpha$ SMA (Fig. 5J\*,K\*). The mesenchymal wall of the pulmonary trunk, but not of the aorta, weakly expresses the cardiac transcription factor NKX2-5 (Fig. 7H). The smooth muscular walls of the arterial trunks express ISL1 (Fig. 7G), reflecting ongoing addition of new cells to the arterial pole of the heart from the pharyngeal mesoderm, but now as smooth muscle cells (Waldo et al. 2005). The loose mesenchyme between the intrapericardial arterial trunks is contiguous with the tissue surrounding the developing trachea and esophagus. It is negative for ISL1, SOX9 and  $\alpha$ SMA, but expresses AP2 $\alpha$  (Figs 5J\*,7G,J), similar to the mesenchymal protrusion seen at stage 16. The walls of the arterial trunks are largely negative for AP2 $\alpha$ , with the facing parts of the walls expressing weakly this factor (Fig. 7J), suggesting their origin from the neural crest-derived mesenchyme of the protrusion. The developing ascending aorta now connects only to the fourth pair of aortic arch arteries (Fig. 7A–C). The pulmonary trunk connects to the sixth aortic arch arteries, which now form its bifurcation. The right-sided arch artery distal to the origin of the right pulmonary artery has almost regressed, while the left-sided arch is enlarged, and is recognisable as the arterial duct (Fig. 7B). The mesenchymal tissue within the distal outflow tract takes the form of the future leaflets of the developing arterial valves, which express SOX9 but, at this stage, only weakly  $\alpha$ SMA (Fig. 5J,J\*,K,K\*). At this stage there are no clear differences in gene expression in the mesenchyme making up the three leaflets of either developing arterial valve (not shown).



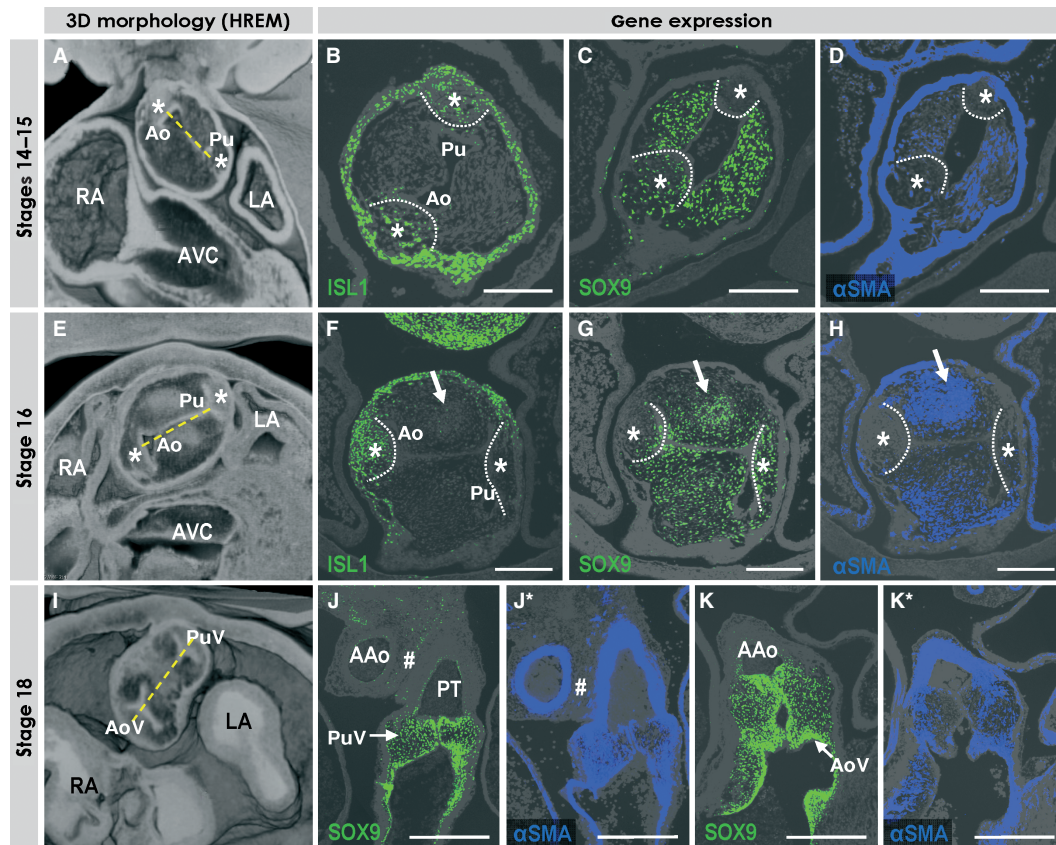


**Fig. 5** The images show the appearance and development of the arterial valves. (A, E, I) Ventral views of the near frontal cuts through the high-resolution episcopic microscopy (HREM) datasets of the embryos at consecutive stages taken through the middle portion of the intrapericardial outflow tract. Note the considerable rotation of the line between aortic (Ao) and pulmonary (Pu) arterial channels. (B–D) Sections of stages 14–15 embryos through the intrapericardial extension of the non-myocardial components derived from the pharyngeal mesenchyme (asterisks, outlined by dotted lines), which were incubated with antibodies as indicated. Note that these extensions are positive for SOX9 and ISL1, while being negative for  $\alpha$ SMA. The arrows point to the cellular condensations within one of the outflow tract cushions (see text). (F–H) Sections of the stage 16 embryo, showing the appearance of the intercalated cushions (asterisks, outlined by dotted lines) within the middle portion of the outflow tract, which were incubated with antibodies as indicated. The intercalated cushions only weakly express ISL1, while beginning to express SOX9 and remaining negative for  $\alpha$ SMA. (J, J\*, K, K\*) Sections through the developing pulmonary (PuV) and aortic (AoV) valves in the stage 18 embryonic heart, which were incubated with antibodies as indicated. The developing leaflets of the valves scarcely express  $\alpha$ SMA, but are strongly positive for SOX9. The tissue between the discrete and separate walls of the arterial trunks (#) is now negative for  $\alpha$ SMA. Scale bars: 200  $\mu$ m.

## Discussion

Experimental studies in animal models have demonstrated that distinct cell populations play an important role in the development of the outflow tract, albeit often neglecting to place the findings into a proper morphological context. All studies on the development of the arterial pole in the human heart, while showing comprehensively the complex morphology of the developing structures (Anderson et al. 2003; Webb et al. 2003), have thus far remained descriptive, as no gene expression data were available. Moreover, the curved form of the pharyngeal region of the growing embryo has rendered unambiguous descriptions of the developing cardiac outflow tract very difficult, requiring a complex terminology system. As recently reviewed (Okamoto

et al. 2010), the extant literature can be quite inaccessible. In this study, we present a 3D and molecular analysis of the dynamic changes that occur during the development of the outflow tract in the human heart. We show that, during stages 14–16, separation of the aortic and pulmonary channels occurs through fusion of the outflow tract cushions with each other and with an intrapericardial protrusion of pharyngeal mesenchyme, constituting initially the dorsal wall of the aortic sac. This protrusion, although neglected recently, had already been recognised in the first half of the previous century as the aortopulmonary septum (Tandler, 1912; Kramer, 1942). We show that in human, as in mouse and chicken, the separate walls of the intrapericardial arterial trunks are formed through addition of ISL1-positive mesenchymal cells to the distal outflow tract. The

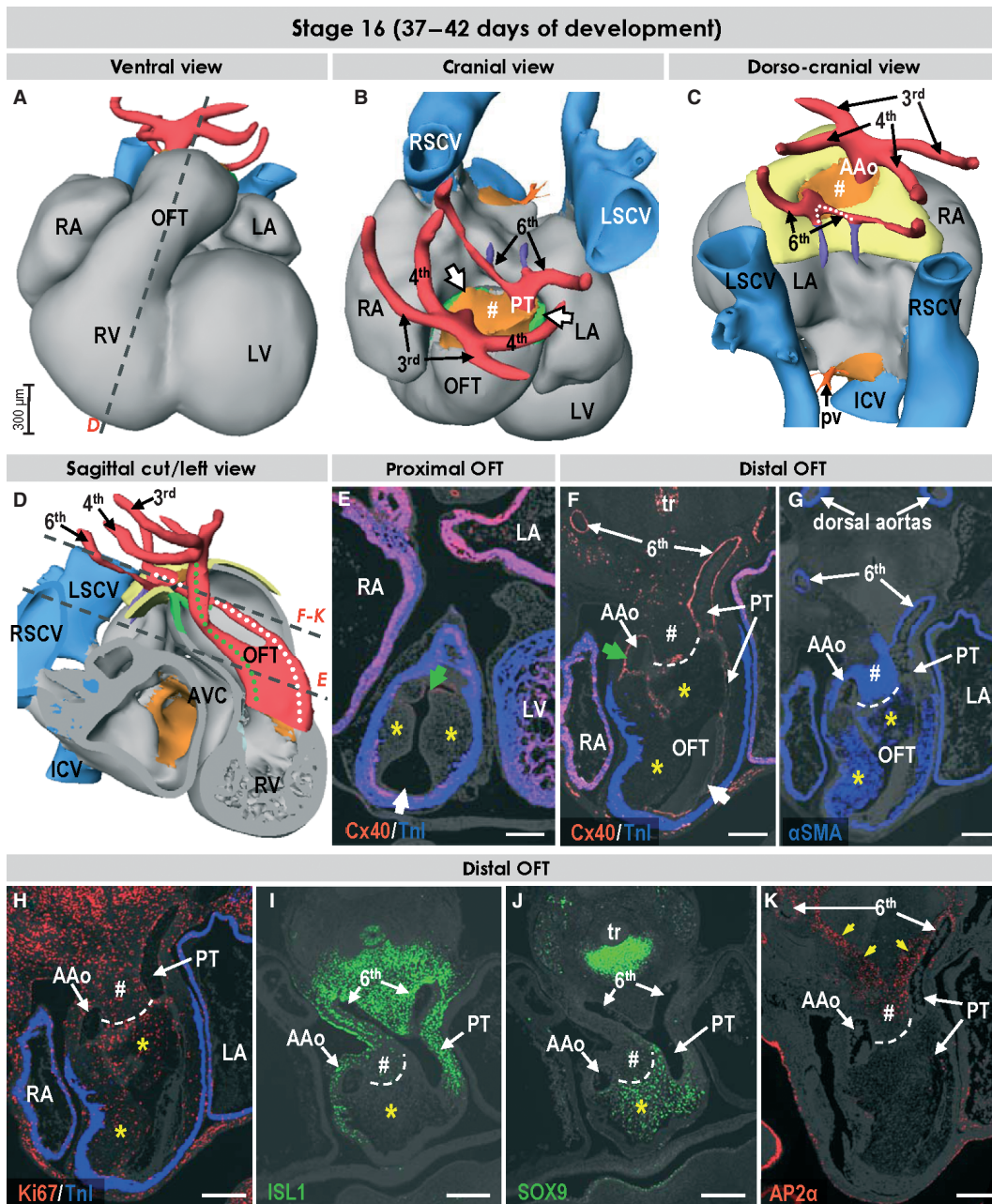


**Fig. 6** Three-dimensional (3D) and molecular analysis of the cardiac outflow tract at stage 16. (A–C) The muscular outflow tract has further shortened, and the mass of the right ventricle is recognisable ventrally. The extrapericardial portions of the perpendicularly oriented ascending aorta and pulmonary trunk are separated from each other by mesenchymal tissue (# in B,C). The dotted line in (C) points to the decreasing distance between the origin of the pulmonary arterial branches. (D) The relations between developing ascending aorta and pulmonary trunk (white and green dotted lines, respectively) now resemble the situation seen in the formed heart. (E) Section through the proximal outflow tract showing the still unused endocardial cushions producing aortic and pulmonary arterial channels (green and white arrows, respectively). (F–K) Sections through the distal outflow tract, which were incubated with antibodies as indicated. The protrusion from the dorsal wall of the aortic sac now extends into the pericardial cavity (#), and interposes between the ascending aorta and the pulmonary trunk. The contact between the protrusion and the distal ends of the outflow tract cushions expressing SOX9 (yellow asterisks) is marked by a dashed line. The yellow arrows in (J) point to the sharp border of the AP2α expression domain. Scale bars: 200 μm. For abbreviations, see previous figures.

morphogenetic steps, along with the gene expression patterns reported in this study, are comparable to those reported for mouse and chicken, and confirm the contribu-

tion of three sources of mesenchyme; endocardium, pharyngeal mesoderm and neural crest, to the shaping of the outflow tract. This involvement of several mesenchymal



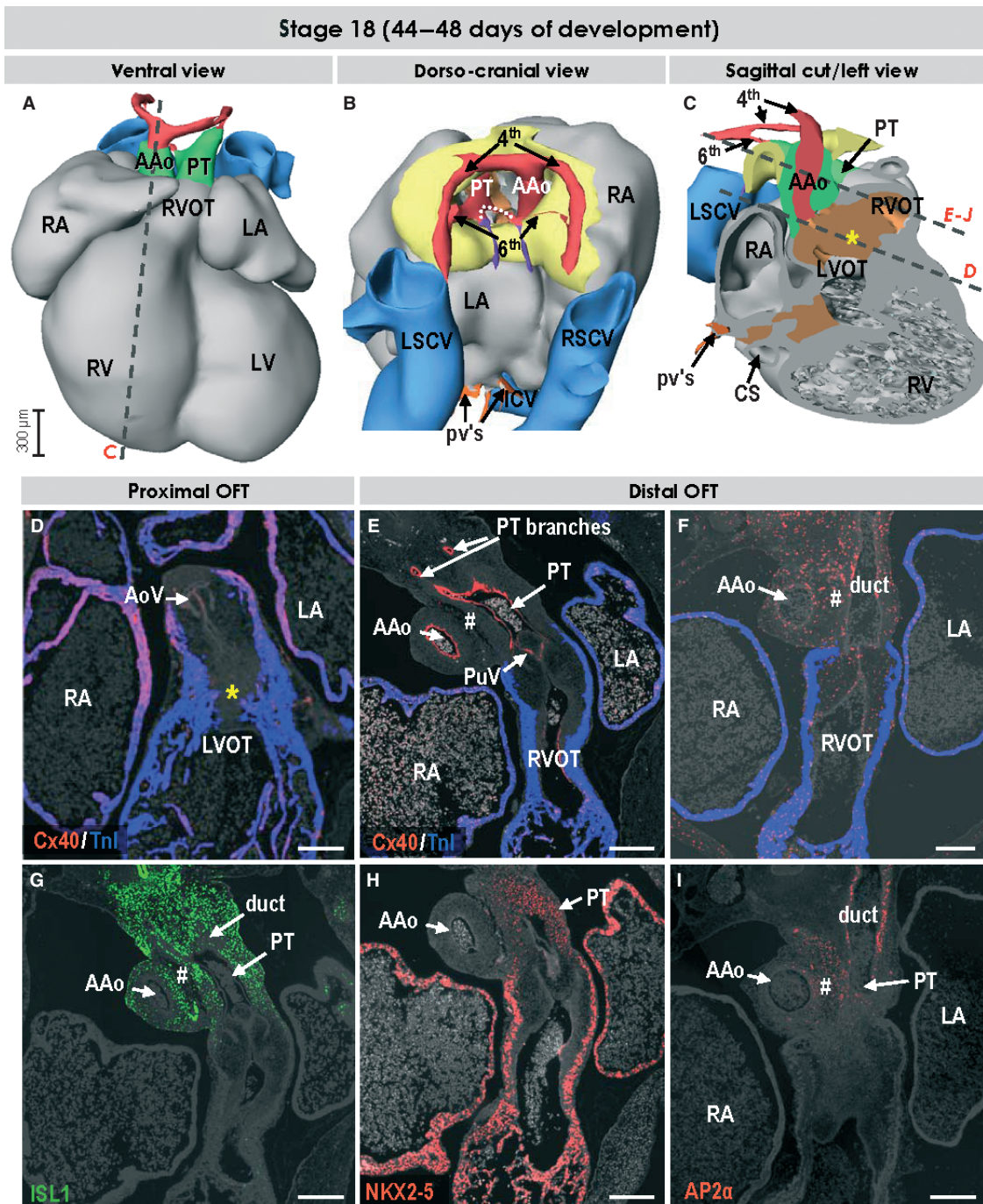


**Fig. 7** Three-dimensional (3D) and molecular analysis of the cardiac outflow tract at stage 18. (A–C) The myocardial outflow tract has further shortened, along with formation of the right ventricular infundibulum (RVOT). The intrapericardial ascending aorta and pulmonary trunk now possess their own discrete non-myocardial walls. The dotted line in (B) points to the proximal parts of the 6th arches, which now form the bifurcation of the pulmonary trunk. The left-sided 6th arch is persisting to become the arterial duct, while the right-sided 6th arch distal to the origin of the right pulmonary artery is regressing. Both 4th arches are of roughly equal size, while the third arches are no longer recognisable. (D) Section through the left ventricular outflow tract (LVOT) and developing aortic valve (AoV). The asterisks in (C) and (D) refer to the myocardialising mesenchyme between the ventricular outflow tracts. (E–J) Sections through the right ventricular outflow tract, developing pulmonary valve (PuV), pulmonary trunk and ascending aorta were incubated with antibodies as indicated. The tissue between great arteries (#) is ISL1-negative and expresses AP2 $\alpha$ , which is also expressed in the facing walls of the arterial trunks. In contrast to the wall of the ascending aorta, the pulmonary truncal wall expressed transcription factor NKX2-5, reflecting the cardiogenic potential of these mesenchymal cells. Scale bars: 200  $\mu$ m. For abbreviations, see previous figures.



tissues of different origin in the development of the cardiac outflow tract correlates well with the great variety of malformations involving the arterial pole of the formed heart, as demonstrated in many studies using animal models.

### Septation of the cardiac outflow tract and establishment of correct ventriculo-arterial connections

Subsequent to the initiation of chamber formation, differentiating cells from the ISL1-positive cardiac progenitor pool continue to be added to the arterial and venous poles of the heart (Cai et al. 2003; Buckingham et al. 2005). At the arterial pole, this contribution initially produces a relatively long, serpentine-like outflow tract with the solitary lumen. One of the most controversial issues remains the mechanism of division of the single lumen of the distal outflow tract into the left and right ventricular outlets. In contrast to the simple concept of the earlier accounts (Tandler, 1912; Kramer, 1942), which recognised the role of the protruding dorsal wall of the aortic sac in the formation of the aortopulmonary septum, the later studies, based on the distinct clustering of mesenchymal cells within the distal outflow tract, assigned the leading role in septation either to the aortopulmonary septal complex, exclusively to the endocardial cushions containing the so-called whorl and prongs, or to a combination of these structures (reviewed in Webb et al. 2003).

Our 3D analysis, facilitated by molecular stainings, reveals several morphogenetic processes occurring at consecutive developmental stages, albeit partly overlapping. The immu-

nohistochemical analyses reveal substantial molecular diversity in the mesenchymal tissues participating in the division of the developing outflow tract of the human heart. The cushion tissue expresses transcription factor SOX9, which is known to be crucial for the formation of intra-cardiac mesenchyme (Akiyama et al. 2004). The mesenchyme of the cushions, which in the mouse and chicken becomes densely populated with neural crest-derived cells (Kirby et al. 1983; Jiang et al. 2000; de Lange et al. 2004), is negative for ISL1, and moderately expresses  $\alpha$ SMA, along with the proliferation marker Ki67. At stage 13, we observed expression of AP2 $\alpha$  within the loose mesenchyme of the most distal part of the outflow tract, and in the mesenchyme surrounding the pharyngeal pouches, which reflects the route of migration of the cardiac neural crest cells toward the cardiac outflow tract (Jiang et al. 2000; Boot et al. 2003). The cushion tissue proximal to the myocardial border of the outflow tract, however, does not express AP2 $\alpha$ , supporting the notion that the neural crest-derived cells no longer express AP2 $\alpha$  as migration ceases (Brewer et al. 2002). The strict complementarity of the expression domains of AP2 $\alpha$  and ISL1 in the pharyngeal mesenchyme shows that the migrating neural crest-derived cells do not mix with the mesenchyme forming the second heart field (Figs 3I,K and 6I,K).

The unseptated tubular outflow tract of the embryonic heart at stages 12 and 13 continues within the pharyngeal mesenchyme as the aortic sac. Unlike a previous report on human embryos (Congdon, 1922), we were unable to find such a structure in human embryos older than stage 14. Between stages 14 and 15, the initial sac is remodeled through intrapericardial protrusion of an oblique septum,

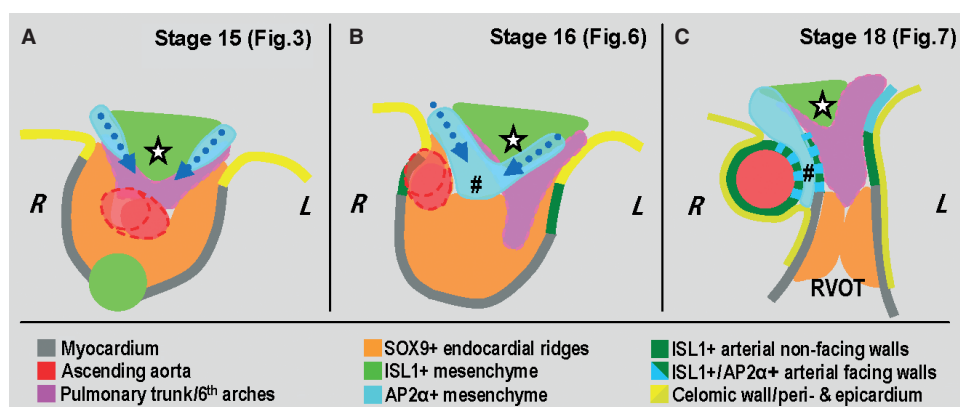


**Fig. 8** Schematic summary of the processes leading to septation of the distal outflow tract. Note that this is a highly simplified 2D view of the morphologically complex 3D structure. (A) At stages 14 and 15, the aortopulmonary foramen within the distal outflow tract is bordered dorsally by ISL1-positive mesenchyme, which gives rise to the extrapericardial 6th aortic arches and the future ascending aorta. At both sides of this ISL1-positive mesenchyme, neural crest-derived cells are migrating ventrally along and cranial to the 6th aortic arches. (B) At stage 16, the endocardial cushions have been formed and fused in the outflow tract to separate the developing aortic and pulmonary channels. Progressive protrusion of the neural crest-derived mesenchyme results initially in the formation of an obliquely oriented aortopulmonary septum (#), and subsequent closure of the aortopulmonary foramen. (C) At stage 18, the continuous addition of ISL1-positive cells at the arterial pole results in the formation of the intrapericardial arterial trunks, the facing walls of which are formed from neural crest-derived mesenchyme. The stars in (A–C) point to the ISL1-positive mesenchyme at the level of the sixth aortic arches, which remains interposed between them. Abbreviations: L/R, left/right; RVOT, right ventricular infundibulum.

causing a rightward shift of the ascending aorta and a leftward shift of the pulmonary trunk and sixth aortic arches (summarised in Fig. 8). This protruding mesenchymal structure had previously been termed the aortopulmonary septum (Kramer, 1942; Tandler, 1912; van Mierop et al. 1963; Rychter, 1978; Orts-Llorca et al. 1982; Beall & Rosenquist, 1990), albeit that it loses its septal identity as the intrapericardial arterial trunks develop their own discrete walls. Identification of the cellular condensations within the fused endocardial cushions, and failure to make a difference between septation within the proximal outflow tract and separation of the intrapericardial arterial trunks, subsequently led to the suggestion of the existence of an aortopulmonary septal complex (Thompson et al. 1985), made up by the so-called whorl and its prongs. Although we have demonstrated such condensations within the outflow cushions (Fig. 5), we found no evidence to support the notion that they play a part in separating the intrapericardial arterial trunks. Our findings show the protruding wall of the aortic sac to fulfill the function of aortopulmonary septation. Our interpretation is compatible with previous labeling studies showing that initial septation of the distal outflow tract involves intrapericardial migration of peribranchial mesenchyme along the sixth aortic arches (Rychter, 1978). A recent study of the Ripply3-deficient mice underscores the importance and sufficiency of such a migration. These mice display complete absence of the third and fourth aortic arches, but have separated intrapericardial arterial trunks, along with normally formed sixth arches (Okubo et al. 2011).

### Formation of the intrapericardial arterial trunks and arterial valves

The intrapericardial outflow tracts of the formed heart distal to the arterial valvar leaflets have walls composed almost exclusively of arterial smooth muscle (Webb et al. 2003). When initially formed, nonetheless, the outflow tract of the developing human heart possesses a solitary lumen and has a complete myocardial wall. Then, as early as stage 16, the orientation of the developing left and right ventricular outlets resembles already the definitive arrangement of the separate, and correctly aligned, left and right ventricular outlets. At this stage, the arterial channels are still largely surrounded by a myocardial wall, the lateral aspects of which possess already a non-myocardial phenotype. Two stages later, as in chicken (Waldo et al. 2005), the separate walls of the intrapericardial arterial trunks are formed distal to the arterial valves by the continuous addition of ISL1-positive cells, differentiating into smooth muscle cells. In the stage 18 embryonic human heart, we observed ISL1 expression in the walls of the intrapericardial arterial trunks, suggesting conservation of the mechanism of their formation in human. The facing walls of the arterial trunks, however, were also positive for AP2 $\alpha$ , indicating a neural crest

origin (Boot et al. 2003). The presence of an intrapericardial arterial wall, along with a common valve, in the setting of common arterial trunk (Russell et al. 2011) shows that addition of ISL1-positive cells and development of valvar leaflets can occur without neural crest-mediated septation of the outflow tract. In line with this is the virtually complete absence of neural crest-derived cells in the leaflets of the mature arterial valves in the mouse, as has been shown by lineage studies (de Lange et al. 2004).

With completion of septation the large portion of the distal outflow tract is occupied by a bulky mass of moderately proliferating cushion tissue making up the arterial valvar primordia. The myocardial wall of the outflow tract, in turn, shows no proliferation, underscoring the discrepancy between growth of the mesenchymal and myocardial tissues at the arterial pole of the developing heart. In human, the development of the arterial valves has been scarcely documented. Thus, the facing leaflets of both arterial valves are presumed to develop from the fused outflow tract cushions, with the remaining leaflets derived from the paired intercalated cushions, or swellings (Kramer, 1942; Maron & Hutchins, 1974). The outflow tract cushions, originating through invasion of endocardium-derived mesenchymal cells into the cardiac jelly (Markwald et al. 1977), are known to become populated by the neural crest-derived cells migrating intrapericardially from outside the heart (Kirby et al. 1983; Jiang et al. 2000).

The origin of the intercalated cushions, however, is not clear and remains to be established. The similar anatomical position of the intrapericardial extensions of the column-like structures, seen at stages 14 and 15, and the intercalated cushions at later stages, suggests a similar origin (Fig. 5). The ISL1-positive pharyngeal mesenchyme, which migrates intrapericardially, and takes the form of two clearly recognisable column-like structures indenting the wall of the distal outflow tract, has received very little previous attention, albeit being clearly documented in the past (Kramer, 1942; de Vries & de Saunders, 1962; Thompson et al. 1985). These mesenchymal columns possess a distinct molecular phenotype, expressing ISL1, but being devoid of SOX9, AP2 $\alpha$  and  $\alpha$ SMA. Such a phenotype is also present in the intercalated cushions, which suggests that the intrapericardially migrating ISL1-positive pharyngeal mesenchyme may form the precursors of the intercalated cushions, which then form the non-facing leaflets of the arterial valves. This, however, remains to be proved by lineage studies in animal models. At later stages, we observed no differences in gene expression between the different leaflets of the developing arterial valves.

### Acknowledgements

We are indebted to the personnel of the Gynaecology Department of the Tartu University Hospital, to Dr M. Aunapuu and Prof. A. Arend from the Anatomy Institute of the University of

Tartu, Estonia, for their help with the collection of the human embryos. We thank J. Hagoort for his continuous support and invaluable help with the preparation of the interactive 3D-PDF file. We thank Dr M.B.J. van den Hoff, Prof. D.J. Henderson and Dr B. Chaudhry for stimulating scientific discussions and support. This work was supported by the European Community's Framework Programmes' contracts LSHM-CT-2005-018630 ('HeartRepair') and Health-F2-2008-223040 ('CHearTED'). Collection of human embryonic material was supported by grant 7301 from the Estonian Science Foundation.

## Author contributions

A.S. performed the collection of the human embryos, the immunofluorescence studies on serial sections, completed the 3D reconstructions and drafted the manuscript. T.J.M. performed the high-resolution episcopic microscopy studies on human embryos. T.J.M., R.H.A., N.A.B. and W.H.L. have provided intellectual input, and helped with editing the manuscript. A.F.M.M. drafted and completed the manuscript and supervised the project.

## References

- Akiyama H, Chaboissier M-C, Behringer RR, et al. (2004) Essential role of Sox9 in the pathway that controls formation of cardiac valves and septa. *Proc Natl Acad Sci USA* **101**, 6502–6507.
- Anderson RH, Webb S, Brown NA, et al. (2003) Formation of the ventricular outflow tracts, arterial valves, and intrapericardial arterial trunks. *Heart* **89**, 1110–1118.
- Beall AC, Rosenquist TH (1990) Smooth muscle cells of neural crest origin form the aorticopulmonary septum in the avian embryo. *Anat Rec* **226**, 360–366.
- Bergwerff M, Verberne ME, DeRuiter MC, et al. (1998) Neural crest cell contribution to the developing circulatory system: implications for vascular morphology. *Circ Res* **82**, 221–231.
- Bettens E, Liu Y, Kjaeldgaard A, et al. (2010) Analysis of early human neural crest development. *Dev Biol* **344**, 578–592.
- de Boer BA, Soufan AT, Hagoort J, et al. (2011) The interactive presentation of 3D information obtained from reconstructed datasets and 3D placement of single histological sections with the 3D portable document format. *Development* **138**, 159–167.
- Boot MJ, Gittenberger-De Groot AC, Iperen L, et al. (2003) Spatiotemporally separated cardiac neural crest subpopulations that target the outflow tract septum and pharyngeal arch arteries. *Anat Rec* **275**, 1009–1018.
- Brewer S, Jiang X, Donaldson S, et al. (2002) Requirement for AP2 $\alpha$  in cardiac outflow tract morphogenesis. *Mech Dev* **110**, 139–149.
- Buckingham ME, Meilhac S, Zaffran S (2005) Building the mammalian heart from two sources of myocardial cells. *Nat Rev Genet* **6**, 826–835.
- Cai CL, Liang X, Shi Y, et al. (2003) Isl1 identifies a cardiac progenitor population that proliferates prior to differentiation and contributes a majority of cells to the heart. *Dev Cell* **5**, 877–889.
- Congdon ED (1922) Transformation of the aortic-arch system during the development of the human embryo. *Contrib Embryol* **14**, 47–113.
- de la Cruz VM, Sanchez-Gomez C, Arteaga MM, et al. (1977) Experimental study of the development of the truncus and the conus in the chick embryo. *J Anat* **123**, 661–686.
- Dyer L, Kirby ML (2009) The role of secondary heart field in cardiac development. *Dev Biol* **336**, 137–144.
- Farrell M, Waldo K, Li YX, et al. (1999) A novel role for cardiac neural crest in heart development. *Trends Cardiovasc Med* **9**, 214–220.
- Gasser RF (1975) Atlas of Human Embryos. London: Harper and Row.
- van den Hoff MJB, Moorman AFM, Ruijter JM, et al. (1999) Myocardialization of the cardiac outflow tract. *Dev Biol* **212**, 477–490.
- Hoffman JL, Kaplan S (2002) The incidence of congenital heart disease. *J Am Coll Cardiol* **39**, 1890–1900.
- Jiang X, Rowitch DH, Soriano P, et al. (2000) Fate of the mammalian cardiac neural crest. *Development* **127**, 1607–1616.
- Kirby ML, Gale TF, Stewart DE (1983) Neural crest cells contribute to normal aorticopulmonary septation. *Science* **220**, 1059–1061.
- Kramer TC (1942) The partitioning of the truncus and conus and the formation of the membranous portion of the inter-ventricular septum in the human heart. *Am J Anat* **71**, 343–370.
- de Lange FJ, Moorman AFM, Anderson RH, et al. (2004) Lineage and morphogenetic analysis of the cardiac valves. *Circ Res* **95**, 645–654.
- Markwald RR, Fitzharris TP, Manasek FJ (1977) Structural development of endocardial cushions. *Am J Anat* **148**, 85–119.
- Maron BJ, Hutchins GM (1974) The development of the semilunar valves in the human heart. *Am J Pathol* **74**, 331–344.
- van Mierop LHS, Alley RD, Kausel HW, et al. (1963) Embryology of the ventricles and great arteries. *Am J Cardiol* **12**, 216–225.
- Okamoto N, Akimoto N, Hidaka N, et al. (2010) Formal genesis of the outflow tracts of the heart revisited: previous works in the light of recent observations. *Congenit Anom (Kyoto)* **50**, 141–158.
- Okubo T, Kawamura A, Takahashi J, et al. (2011) Ripply3, a Tbx1 repressor, is required for development of the pharyngeal apparatus and its derivatives in mice. *Development* **138**, 339–348.
- O'Rahilly R, Müller F (1987) Developmental Stages in Human Embryos. Including a revision of Streeter's "Horizons" and a survey of the Carnegie Collection. Washington: Carnegie Institution Washington, publication 647.
- Orts-Llorca F, Puerta-Fonolla J, Sobrado J (1982) The formation, septation and fate of the truncus arteriosus in man. *J Anat* **134**, 41–56.
- Rana MS, Horsten NC, Lamers WH, et al. (2007) Trabeculated right ventricular free wall in the chicken heart forms by ventricularization of the myocardium initially forming the outflow tract. *Circ Res* **100**, 1000–1007.
- Russell HM, Jacobs ML, Anderson RH, et al. (2011) A simplified categorization for common arterial trunk. *J Thorac Cardiovasc Surg* **141**, 645–653.
- Rychter Z (1978) Analysis of relations between aortic arches and aortico-pulmonary septation. In: *Morphogenesis and malformation of the cardiovascular system. Birth Defects: Original Article Series*, Vol. 14. No. 7 (eds Rosenquist G, Bergsma D), pp. 443–448. New York: Alan R. Liss.
- Samánek M (1992) Children with congenital heart disease: probability of natural survival. *Pediatr Cardiol* **13**, 152–158.
- Sizarov A, Anderson RH, Christoffels VM, et al. (2010) Three-dimensional and molecular analysis of the venous pole of the developing human heart. *Circulation* **122**, 798–807.



- Tandler J** (1912) The development of the heart. In: *Manual of Human Embryology*, Vol. II. (eds Keibel F, Mall FP), pp. 534–569. Philadelphia: Lippincott Company.
- Thompson RP, Sumida H, Abercrombie V, et al.** (1985) Morphogenesis of the human cardiac outflow. *Anat Rec* **213**, 578–586.
- de Vries PA, de Saunders JB** (1962) Development of the ventricles and spiral outflow tract in the human heart. A contribution to the development of the human heart from age group IX to age group XV. *Contrib Embryol* **37**, 89–114.
- Waldo KL, Hutson MR, Ward CC, et al.** (2005) Secondary heart field contributes myocardium and smooth muscle to the arterial pole of the developing heart. *Dev Biol* **281**, 78–90.
- Webb S, Qayyum SR, Anderson RH, et al.** (2003) Septation and separation within the outflow tract of the developing heart. *J Anat* **202**, 327–342.
- Weninger WJ, Mohun TJ** (2007) Three-dimensional analysis of molecular signals with episcopic imaging techniques. *Methods Mol Biol* **411**, 35–46.

- Ya J, van den Hoff MJB, Franco D, et al.** (1998) Normal development of the outflow tract. *Circ Res* **82**, 464–472.

## Supporting Information

Additional supporting Information may be found in the online version of this article.

**Data S1.** Interactive 3D-PDF file. The 3D reconstructions of the embryonic hearts and vessels at four consecutive stages presented in the interactive format, which permit the reader to form his or her independent opinion.

As a service to our authors and readers, this journal provides supporting information supplied by the authors. Such materials are peer-reviewed and may be re-organized for online delivery, but are not copy-edited or typeset. Technical support issues arising from supporting information (other than missing files) should be addressed to the authors.